Vol. 32 (2001) ACTA PHYSICA POLONICA B No 10 Special Issue

SHORT COHERENCE LENGTH SUPERCONDUCTORS WITH ANISOTROPIC PAIRING IN 2D*

R. MICNAS AND B. TOBIJASZEWSKA

Institute of Physics, A. Mickiewicz University
Umultowska 85, 61-614 Poznań, Poland

(Received June 21, 2001)

The two models of short coherence length superconductors with anisotropic pairing symmetry are discussed. First, we examine superconducting properties of the extended Hubbard model with intersite attraction on a 2D square lattice with nearest- and next-nearest-neighbor hopping. The effects of phase fluctuations on the extended s and $d_{x^2-y^2}$-wave as well as on the mixed $s\pm id$ state are studied within the Kosterlitz–Thouless scenario. This leads to a new phase with a pseudogap, and the universal linear scaling of the critical temperature *versus* zero temperature phase stiffness can occur on the Uemura type plots due to the separation of scales for pairing and for the phase coherence. The second model is that of local electron pairs and itinerant fermions coupled via charge exchange mechanism, which mutually induces superconductivity in both subsystems. The phase diagram of this two-component system is presented for anisotropic pairing on a 2D square lattice.

PACS numbers: 74.20.–z, 71.10.Fd, 74.20.Mn, 74.72.–h

1. Introduction

The cuprate High Temperature Superconductors (HTS) are strongly anisotropic systems. The short coherence length and low superfluid density in the underdoped regime indicate that phase fluctuations are important [1,2]. In this paper we briefly outline properties of two models of short-coherence length anisotropic superconductors with emphasis on the role played by thermal phase fluctuations of the order parameter.

* Presented at the XII School of Modern Physics on Phase Transitions and Critical Phenomena Lądek Zdrój, Poland, June 21–24, 2001.

2. The extended Hubbard model with intersite attraction

The simplest model which describes both extended s-wave (s^*) and $d_{x^2-y^2}$-wave pairing symmetries is the extended Hubbard model with on-site repulsion and intersite attraction [3–5]:

$$H = \sum_{ij,\sigma}(t_{ij} - \mu\delta_{ij})c^\dagger_{i\sigma}c_{j\sigma} + \frac{1}{2}U\sum_{i\sigma} n_{i\sigma}n_{i-\sigma} + \frac{1}{2}\sum_{ij,\sigma\sigma'} W_{ij}n_{i\sigma}n_{j\sigma'}, \qquad (1)$$

where $n_{i\sigma} = c^\dagger_{i\sigma}c_{i\sigma}$, t_{ij} is the transfer integral, μ the chemical potential, U is the on-site and W_{ij} is the intersite interaction. In our analysis we consider $W < 0$ *i.e.* the case of nearest neighbor attraction. Comprehensive studies of the anisotropic superconductivity, the competition between d-wave superconductivity and antiferromagnetism on 2D lattice as well as the effects of phase fluctuations in the model (1) have been performed in Refs. [3–8]. Here we focus on the phase diagrams including a possibility of $s \pm id$ symmetry mixing, the role of phase fluctuations and analyze the Uemura type plots. Within the Hartree-Fock-BCS approximation (BCS-HFA) the energy gap is determined by the equation:

$$\Delta_{\vec{k}} = \frac{1}{N}\sum_{\vec{q}}(-U - W_{\vec{k}-\vec{q}})\Delta_{\vec{q}}F_{\vec{q}}, \qquad (2)$$

where $F_{\vec{q}} = \frac{1}{2E_{\vec{q}}}\tanh(\frac{\beta E_{\vec{q}}}{2})$, $W_{\vec{k}}$ is the Fourier transform of W_{ij} and $\beta = 1/k_{\rm B}T$. The quasiparticle energy is given by $E_{\vec{q}} = \sqrt{\bar{\varepsilon}^2_{\vec{q}} + |\Delta_{\vec{q}}|^2}$, $\bar{\varepsilon}_{\vec{q}} = \varepsilon_{\vec{q}} - \bar{\mu}$, where the electron dispersion on a 2D square lattice is $\varepsilon_q = -2t(\cos(q_xa) + \cos(q_ya)) - 4t_2\cos(q_xa)\cos(q_ya)$ with the next nearest neighbor (nnn) hopping parameter t_2, and $\bar{\mu} = \mu - n(U/2 + 4W)$. In the case of singlet pairing the gap function takes the form: $\Delta_{\vec{k}} = \Delta_0^s + \Delta_\gamma\gamma_{\vec{k}} + \Delta_\eta\eta_{\vec{k}}$, where $\gamma_{\vec{k}} = 2(\cos(k_xa) + \cos(k_ya))$ and $\eta_{\vec{k}} = 2(\cos(k_xa) - \cos(k_ya))$. The first and second terms refer to the on-site and extended s-wave (s^*) and the third one to the $d_{x^2-y^2}$-wave pairing. The resulting equations for the gap amplitudes are solved together with the equation determining the chemical potential $\bar{\mu}$: $n - 1 = -\frac{2}{N}\sum_{\vec{k}}\bar{\varepsilon}_{\vec{k}}F_{\vec{k}}$. n is the electron concentration.

If the states with pure s^*-wave (assuming $U = 0$)($\Delta_\gamma \neq 0$, $\Delta_\eta = 0$) and d-wave (with $\Delta_\eta \neq 0$, $\Delta_\gamma = 0$) symmetry overlap a mixed symmetry state can appear. The free energy calculations show, that for systems with the tetragonal symmetry, $s^* \pm id$ phase (with $\Delta_{\vec{k}} = \Delta_\gamma\gamma_{\vec{k}} \pm i\Delta_\eta\eta_{\vec{k}}$ and time-reversal symmetry breaking) is more stable than $s^* \pm d$ phase [8].

The BCS critical temperature ($T_{\rm c}^{\rm BCS}$) is the one at which the gap amplitude vanishes. To include phase fluctuations we apply the Kosterlitz–Thouless (KT) theory. The transition temperature ($T_{\rm c}^{\rm KT}$) is determined by the universal jump of superfluid stiffness ρ_s:

$$\rho_s^-(T_{\rm c}) = \frac{2}{\pi} k_{\rm B} T_{\rm c}, \tag{3}$$

where ρ_s, obtained from the linear response theory, is given by

$$\rho_s(T) = \frac{1}{2N} \sum_{\vec{k}} \left\{ \left(\frac{\partial \varepsilon_{\vec{k}}}{\partial \vec{k}_\alpha} \right)^2 \frac{\partial f(E_{\vec{k}})}{\partial E_{\vec{k}}} + \frac{1}{2} \frac{\partial^2 \varepsilon_{\vec{k}}}{\partial \vec{k}_\alpha^2} \left[1 - \frac{\overline{\varepsilon}_{\vec{k}}}{E_{\vec{k}}} \tanh\left(\frac{\beta E_{\vec{k}}}{2} \right) \right] \right\} \tag{4}$$

and $f(E_{\vec{k}})$ is the Fermi–Dirac distribution function, $\alpha = x, y, z$. In the local limit $\lambda^{-2} = (16\pi e^2/\hbar^2 c^2)\rho_s$, λ being the London penetration depth.

Numerically determined phase diagram including s^*, d and $s^* + id$ states is shown in Fig. 1. For $|t_2| < 0.5t$, the s^*-wave symmetry occurs for low n and is strongly restricted by the mixed state, while d-wave is stabilized for higher n. In the BCS–HFA the transition from the $s^* + id$ state to the state with pure symmetry is continuous and the four second order phase transition lines meet at the TTCP. The KT temperatures are significantly lower than the $T_{\rm c}^{\rm BCS}$ (Fig. 1). Phase fluctuations destroy superconductivity above $T_{\rm c}^{\rm KT}$ but the pairs are thermally broken only at $T_{\rm c}^{\rm BCS}$. In the region $T_{\rm c}^{\rm KT} < T < T_{\rm c}^{\rm BCS}$ the Cooper pairs exist, but they are phase incoherent. This state characterized by the gap in fermionic spectrum can be responsible for the pseudo-gap phase observed in the underdoped cuprate HTS.

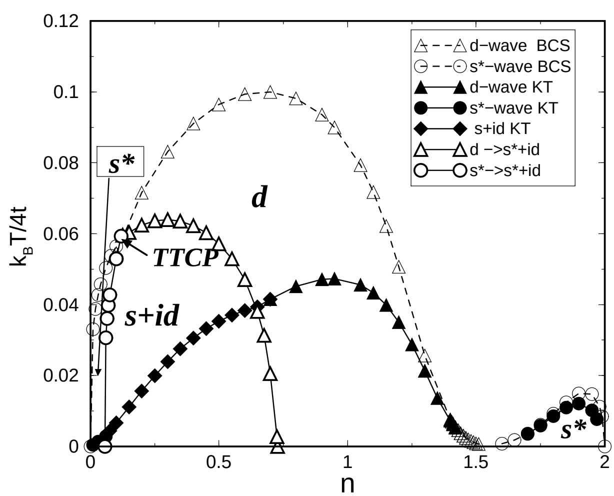

Fig. 1. Phase diagram in $T - n$ plane for $|W|/4t = 0.5$, $t_2 = -0.45t$ ($U = 0$). Filled symbols denote $T_{\rm c}^{\rm KT}$, empty symbols and dashed lines — $T_{\rm c}^{\rm BCS}$, empty symbols and solid lines — borders of mixed $s + id$ phase. TTCP is the tetracritical point.

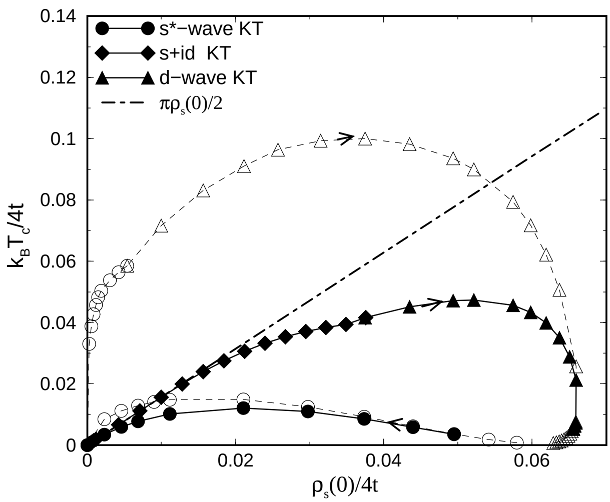

Fig. 2. Uemura type plot with the control parameter n (indicated by arrows), for $|W|/4t = 0.5$, $t_2 = -0.45t$ $(U = 0)$. Solid lines with filled symbols denote $T_{\mathrm{c}}^{\mathrm{KT}}$, dashed lines with empty symbols denote $T_{\mathrm{c}}^{\mathrm{BCS}}$. Open triangle — d-wave BCS, open circle — s^*-wave BCS. The dot-dashed line $\pi\rho_s(0)/2$ is an upper bound on the phase ordering temperature

The Uemura type plots (critical temperatures *vs* $\rho_s(T = 0)$), with the control parameter n, are presented in Fig. 2. It should be noted that the Uemura scaling $T_{\mathrm{c}} \sim 1/\lambda(0)^2$ is not obeyed within the BCS-HFA scheme. In a dilute limit, the KT temperatures points collapse on the universal line $\pi\rho_s(0)/2$, because of separation of the energy scales for pairing and phase coherence (in this region $\Delta(0) \gg \rho_s(0)$). The left s^*-wave branch is restricted to low n, for higher n the $s + id$ state appears, and next pure d-wave state. For $n > 1.45$ the right s^*-wave branch occurs and $\rho_s(0)$ descends to 0 for $n = 2$. Thus, with growing n, the return is on the s^*-wave branch.

It is also of interest to discuss the case of $|t_2| > 0.5t$. In such a case, a pure d-wave pairing can be realized in low densities and competition with s^*-wave symmetry is pushed to higher values of n. In Fig. 3 we show the phase diagram for $t_2/t = -0.7$. We notice the existence of quantum critical point separating the band insulator and d-wave superconductor at $T = 0K$. Its position for $0.5 < |t_2/t| < 1$ is determined by $\bar{\mu} = 4t_2 - E_b/2$, where E_b is the binding energy of d-wave pair in an empty lattice and can be given exactly. In this case the Uemura scaling for d-wave symmetry is obeyed in an extended range of concentrations, due to separation of the scales for the pairing and the phase coherence. However, in low n region the d-wave pairing is nodeless and the transition to d-wave with the nodal points (and

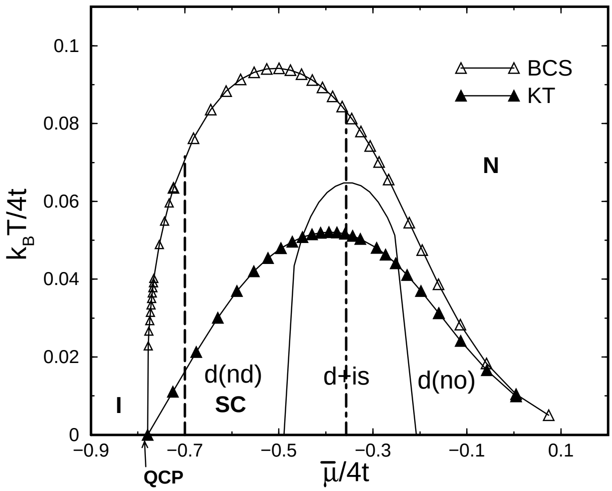

Fig. 3. Phase diagram for $t_2/t = -0.7$, $|W/4t| = 0.5$, in $T - \bar{\mu}$ plane. The range of $\bar{\mu}$ corresponds to n varying from 0 to 1.4. d(nd) — $d_{x^2-y^2}$-wave nodeless phase, d(no) — $d_{x^2-y^2}$-wave with nodal points, $d + is$ — mixed symmetry state, nodeless. The solid line, plotted for $U = 0$ shows stability of $d + is$ state. I-insulator, SC-superconductor, N-normal state. QCP is the Quantum Critical Point. The dashed line marks the crossover from BCS to LP (Local Pair) regimes at $T = 0K$. The dot-dashed line marks a transition from nodeless d-wave state to d-wave with nodal points at $T = 0K$.

the presence of nodal quasiparticles), can take place for higher n. This is in contrast to the case of $|t_2| < 0.5t$, where we have d-wave pairing with four nodal points, and this fact has important consequences for temperature behavior of the superfluid density and spectral properties. Let us point out that a density driven crossover from BCS to Bose condensation of LP pairs can take place for d-wave symmetry (*c.f.* Fig. 3). This crossover is smooth in contrast to the case of d-wave pairing with nodal points, for which the crossover is continuous but not smooth [7, 8].

We should also add that the finite on-site repulsion U will modify the phase diagrams by reducing the s-wave component and the range of stability of mixed symmetry state thus expanding pure d-wave state. Indeed, $U > 0$ will also lead to competition with antiferromagnetic order [3, 8].

In Fig. 4 the results obtained in the KT scenario are compared with experimental ones [8, 9]. For each family of cuprate HTS the experimental $T_{\rm c}$ (being a function of doping) have been scaled to $T_{\rm c}^{\max}$, and $\rho_s(0)$ to the value $\rho_s(0)^{\max}$ attained at $T_{\rm c}^{\max}$. Analogously, the theoretical results given in Fig. 2 (only for $s + id$ and d-wave state) have been scaled. As we see, there is an agreement between experimental points and our theoretical lines. In the underdoped regime the $s+id$ solution is stable, in the optimally doped regime the theory is consistent with $d_{x^2-y^2}$ pairing. The largest deviations are observed in the overdoped regime.

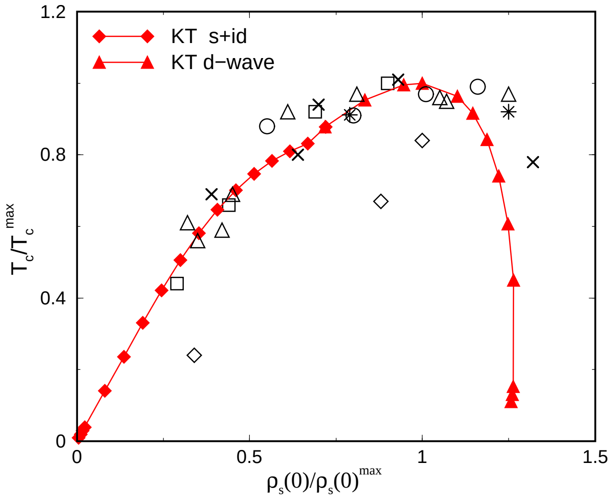

Fig. 4. Comparison of theoretical results (solid lines with filled symbols) from Fig. 2 with the experimental points taken from Ref. [9]. $\times$ —$La_{2-x}Sr_xCuO_4$, $\triangle$ — $YBa_2Cu_3O_x$, $\square$ — $Y_{1-x}Pr_xBa_2Cu_3O_{6.97}$, $\diamond$ — $Tl_2Ba_2CuO_{6+\delta}$, $*$ — $Tl_2Ba_2Ca_2Cu_3O_{10}$, $Tl_{0.5}Pb_{0.5}Sr_2Ca_2Cu_3O_9$, $\circ$ — $Bi_2Sr_2Ca_{1-x}Y_xCu_2O_9$.

3. The two-component model of coexisting local pairs and electrons

A mixture of interacting charged bosons (bound electron pairs) and electrons can show features which are intermediate between those of local pair superconductors and those of classical BCS systems. Such a two-component model has been proposed for high temperature superconductors [10] and recently studied by several authors [10–13]. We shall consider a generalization of the model to the case of anisotropic pairing of extended s-wave or d-wave type, which is defined by the following Hamiltonian

$$H = \sum_{\boldsymbol{k}\sigma}(\varepsilon_{\boldsymbol{k}} - \mu)c^{\dagger}_{\boldsymbol{k}\sigma}c_{\boldsymbol{k}\sigma} \;+\; 2\sum_{i}(\Delta_0 - \mu)b^{\dagger}_i b_i - \sum_{ij} J_{ij} b^{\dagger}_i b_j + \frac{1}{\sqrt{N}}\sum_{\boldsymbol{q}} I(B^{\dagger}_{\boldsymbol{q}} b_{\boldsymbol{q}} + b^{+}_{\boldsymbol{q}} B_{\boldsymbol{q}}), \qquad (5)$$

$\varepsilon_{\boldsymbol{k}}$ refers to the energy band of the c-electrons, Δ_0 measures the relative position of the LP level with respect to the bottom of the c-electron band, μ stands for the chemical potential which ensures that the total number of particles in the system is constant, *i.e.*

$$n = \frac{1}{N}\left(\sum_{\boldsymbol{k}\sigma}\left\langle c^\dagger_{\boldsymbol{k}\sigma}c_{\boldsymbol{k}\sigma}\right\rangle + 2\sum_i \langle b_i^\dagger b_i\rangle\right) = n_{\rm c} + 2n_b\,.$$

J_{ij} is the pair hopping integral.

$$B^\dagger_{\boldsymbol{q}} = \sum_{\boldsymbol{k}} \phi_k c^\dagger_{\boldsymbol{k}+\boldsymbol{q}/2,\uparrow} c^\dagger_{-\boldsymbol{k}+\boldsymbol{q}/2,\downarrow}$$

denotes the singlet pair creation operator of c-electrons and I is the coupling constant. The operators for local pairs (hard-core charged bosons) $b_i^\dagger, b_i$ obey the Pauli commutation rules: $[b_i, b_j^\dagger] = (1-2n_i)\delta_{ij}$, $[b_i, b_j] = 0$, $(b_i^\dagger)^2 = (b_i)^2 = 0$, $b_i^\dagger b_i + b_i b_i^\dagger = 1$, $n_i = b_i^\dagger b_i$. We assume that the coupling between the two subsystems is via the center of mass momenta $\boldsymbol{q}$ of the Cooper pair $B^\dagger_{\boldsymbol{q}}$ and the hard-core boson $b_{\boldsymbol{q}}$. The pairing symmetry, on a 2D square lattice, is determined by the form of ϕ_k, which is 1 for the on-site pairing, $\phi_k = \gamma_{\boldsymbol{k}}$ for the extended s-wave and $\phi_{\boldsymbol{k}} = \eta_{\boldsymbol{k}}$ for the $d_{x^2-y^2}$-wave pairing. In general, one can consider a decomposition $I\phi_k = g_0 + g_s\gamma_k + g_d\eta_k$, with appropriate coupling constants for different symmetry channels.

As in the previous section, our analysis is based on the BCS-Mean-Field Approximation (MFA) and the Kosterlitz–Thouless (KT) theory for two-dimensional superfluid. The direct bosonic hopping J_{ij} is not considered here. The superconducting state is characterized by two order parameters:

$$x_0 = \frac{1}{N}\sum_k \phi_k \langle c^\dagger_{k\uparrow} c^\dagger_{-k\downarrow}\rangle$$

and

$$\rho_0^x = \frac{1}{2N}\sum_i \langle b_i^\dagger + b_i\rangle\,,$$

which satisfy the set of equations:

$$x_0 = -\frac{1}{N}\sum_{\boldsymbol{k}} \frac{I\phi_k^2\rho_0^x}{2E_{\boldsymbol{k}}}\tanh\left(\frac{\beta E_{\boldsymbol{k}}}{2}\right)\,, \tag{6}$$

$$\rho_0^x = -\frac{Ix_0}{2\Delta}\tanh(\beta\Delta)\,, \quad n = n_{\rm c} + 2n_b, \tag{7}$$

where the quasiparticle energy is given by $E_k = \sqrt{\bar{\varepsilon}_k^2 + \Delta_k^2}$, $\bar{\varepsilon}_k = \varepsilon_k - \mu$, $\Delta_{\boldsymbol{k}}^2 = I^2 \phi_k^2 (\rho_0^x)^2$. $\Delta = \sqrt{(\Delta_0 - \mu)^2 + I^2 x_0^2}$. The c-electron dispersion is

$$\varepsilon_k = -2t(\cos(k_x a) + \cos(k_y a)) - 4t_2 \cos(k_x a)\cos(k_y a) - \varepsilon_b\,, \quad \varepsilon_b = \min\varepsilon_k\,.$$

The superfluid density, derived within BCS scheme, is given by

$$\rho_s^\alpha = \frac{1}{2N}\sum_k \left\{ \left(\frac{\partial \varepsilon_k}{\partial k_\alpha}\right)^2 \frac{\partial f(E_k)}{\partial E_k} + \frac{1}{2}\frac{\partial^2 \varepsilon_k}{\partial k_\alpha^2}\left[1 - \frac{\bar{\varepsilon}_k}{E_k}\tanh\left(\frac{\beta E_k}{2}\right)\right]\right\}\,.$$

Finally, the effect of phase fluctuations on the critical temperatures is evaluated within the KT theory, *i.e.*, from the relation for the universal jump of the superfluid stiffness at $T_{\rm c}$ (Eq. (3)).

We have performed an extended analysis of the phase diagrams and superfluid properties of the model (5) for different pairing symmetries [14]. The typical phase diagram (for d-wave symmetry) plotted as a function of the position of LP level Δ_0 is shown in Fig. 5.

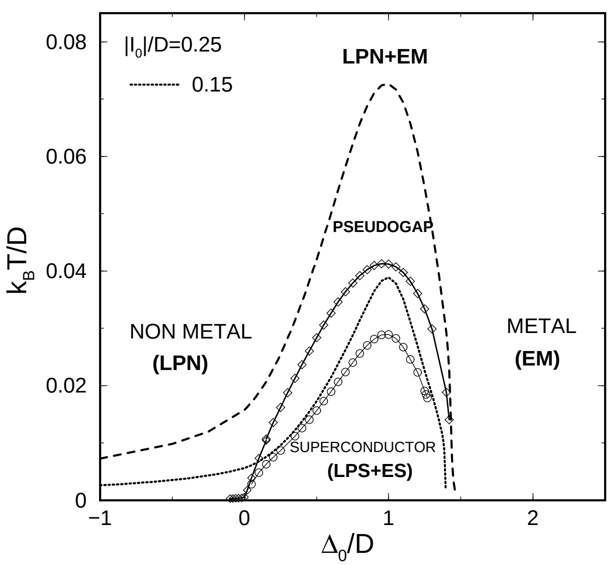

Fig. 5. Phase diagram of the induced pairing model for the $d_{x^2-y^2}$ – wave symmetry and $n = 1.5$. $I = -|I_0|$, $J_{ij} = 0$. $D = 4t$. The dashed line — BCS-MFA transition temperature, the line with diamonds — KT transition temperature, for $|I_0|/D = 0.25$. LPN — nonmetallic phase of LP, EM — electronic metal, LPS+ES -superconducting state. The dotted line and the line with circles show BCS-MFA and KT transition temperatures, respectively, for $|I_0|/D = 0.15$

A sharp drop in the superfluid stiffness (and in the KT transition temperature) occurs when the bosonic level reaches the bottom of the c-electron band and the system approaches the LP limit. In the opposite, BCS like limit, T_c asymptotically approaches the MF transition temperature, with narrow fluctuation regime. Between the KT and MFA temperatures the phase fluctuation effects are important. In this regime a pseudo-gap in c-electron spectrum will develop and the normal state of LP and itinerant fermions can exhibit non-Fermi liquid properties [11].

With varying n but for fixed Δ_0, it appears that the mechanism of induced superconductivity in the mixed regime of coexisting LP and electrons is not very sensitive to the pairing symmetry, *i.e.* n_c is nearly constant, but n_b (LP level occupation) increases with total n. The chemical potential in the superconducting phase is practically pinned around Δ_0. The superfluid density exhibits linear in T behavior (at low T) for $d_{x^2-y^2}$-wave pairing due to the existence of nodal quasiparticles. For the same pairing symmetry, we have also found that the scaled stiffness $\rho_s(T)/\rho_s(0)$ *vs* T/T_c shows only a weak dependence on the total density n. The d-wave pairing is preferred for higher concentration of c electrons, while the extended s-wave can be realized for lower n_c (for the nn hopping). The nnn hopping can substantially enhance T_c for d-wave symmetry. Finally, within the KT scenario, the Uemura-type plots have also been obtained for s^* and d-wave symmetry [14].

B.T. acknowledges partial support by the Polish State Committee for Scientific Research (KBN), Project No. 2 P03B 037 17. Thanks are due to S. Robaszkiewicz and T. Kostyrko for helpful discussions.

REFERENCES

[1] R. Micnas, S. Robaszkiewicz, *High-T_c Superconductivity 1996: Ten Years after the Discovery*, *NATO ASI Appl. Sci.* **E343**, 31 (1997), and references therein.

[2] V.J. Emery, S.A. Kivelson, *Nature* **374**, 434 (1995).

[3] R. Micnas, J. Ranninger, S. Robaszkiewicz, S. Tabor, *Phys. Rev.* **B37**, 9410 (1988).

[4] R. Micnas, J. Ranninger, S. Robaszkiewicz, *Phys. Rev.* **B39**, 11653 (1989).

[5] R. Micnas, S. Robaszkiewicz, B. Tobijaszewska, *J. Supercond.* **12**, 79 (1999).

[6] B. Tobijaszewska, R. Micnas, *Mol. Phys. Rep.* **24**, 236 (1999).

[7] B. Tobijaszewska, R. Micnas *Acta Phys. Pol.* **A97**, 393 (2000).

[8] B. Tobijaszewska, Ph. D. Thesis UAM, Poznań 2001.

[9] Y.J. Uemura *et al.*, *Phys. Rev. Lett.* **62**, 2317 (1989); C. Niedermayer *et al.*, *Phys. Rev. Lett.* **71**, 1764 (1993).

[10] R. Micnas, J. Ranninger, S. Robaszkiewicz, *Rev. Mod. Phys.* **62**, 113 (1990) and references therein.

[11] J. Ranninger, M. Robin, *Phys. Rev.* **B53**, R11961(1996); H.C. Ren, *Physica* **303C**, 115 (1998).

[12] L.P. Gorkov, A.V. Sokol, *JETP Lett.* **46**, 420 (1987); L.P. Gorkov, *J. Supercond.* **14**, 365 (2001).

[13] V.B. Geshkenbein, L.B. Ioffe, A.I. Larkin, *Phys. Rev.* **B55**, 3173 (1997); C.P. Enz, *Phys. Rev.* **B54**, 3589 (1996).

[14] R. Micnas, S. Robaszkiewicz, B. Tobijaszewska, A. Bussmann-Holder, to be published.